IS-T--1476

DE90 011804

The Effect of Manganese on the Onset of the Stage II Reaction in an Austempered Ductile Iron Matrix

by

Kenneth Norman Hagen

MS Thesis submitted to Iowa State University

Ames Laboratory, U.S. DOE

Iowa State University

Ames, Iowa 50011

Date Transmitted: February 1990

PREPARED FOR THE U. S. DEPARTMENT OF ENERGY

UNDER CONTRACT NO. W-7405-Eng-82.

DISCLAIMER

DISCLAIMER

TABLE OF CONTENTS

I. INTRODUCTION

Austempered ductile irons (ADIs) possess a unique combination of toughness and ductility plus high strength which make them attractive alternatives to other metal castings. ADIs can have tensile strengths up to 230 ksi with a 1% elongation and high hardness for wear resistant applications, or tensile strengths of approximately 150 ksi and elongations of 14% where a large amount of ductility is required. The largest use of ADI is for various types of gears; some other applications include crankshafts, camshafts, and railway wagon wheels. According to Hitchcox [1], "the ADI gears are lighter, more machinable, stronger, quieter running, and more economical to manufacture than the forged, carburized steel gears they replace." Some additional examples of ADI use include the Atmosphere Furnace Company's replacement of a forged tool steel tire cutter knife with an ADI knife, Hayes-Albion Corporation's reduction in weight of a road wheel arm by 1/3 by substituting ADI for the previous casting material, and General Motors use of ADI hypoid gears in their Pontiac automobiles. Although cost and weight savings can be significant, simple economics is not the only reason for the success of ADI gears. A major cause of gear failure results from bending fatigue or contact fatigue. The bending fatigue strength and contact strength of shot peened ADI gears is superior to ferritic and pearlitic ductile irons, as well as cast or forged and heat treated steels [1].

Austempering is a two step process: 1) complete transformation to the austenite (γ) phase and 2) a quench and hold in the temperature

range of 270-420° C for some time followed by cooling to room temperature. This quench must be sufficiently rapid to avoid formation of pearlite or ferrite if the best mechanical properties are to be obtained.

There are two basic microstructures in ADI. Ductile irons (DIs) which transform from γ at lower temperatures (270-320° C) contain a lower bainitic structure. This structure has a high hardness (> 400 HRB) and strength and is best suited to high contact stress applications. Transformation at higher temperatures (370-420° C) results in an upper bainitic structure. This structure has a hardness of 260-350 HRB, and combines high ductility and toughness with high fatigue strength and wear resistance, making it a useful material for structural applications such as crankshafts [2].

When ordinary steels are allowed to transform isothermally from γ at a temperature of 270-420° C, bainite (α + cm) is formed. While the classic terms 'upper' and 'lower' bainite are used for the reaction in ADIs, they are not accurate descriptions of the resulting microstructure. This is because the high silicon content of ADIs suppresses the cementite (Fe_3C) phase normally associated with bainite transformations in steels and a ferritic microstructure (called bainitic ferrite) is formed during the isothermal transformation instead. Suppression of the cementite phase causes the remaining austenite to be enriched with carbon, depressing the martensite start temperature (M_S) to well below 0° C. The remaining austenite continues to absorb carbon until the the solid solubility limit is approached and transformation ceases. If the DI is held at this temperature for an extended time, the

high carbon austenite will transform to bainitic ferrite plus carbides. Thus, we observe a two stage reaction. Firstly, austenite (γ_0) decomposes into bainitic ferrite (α) and high carbon austenite (γ_{HC}).

$$\text{Stage I :} \qquad \gamma_0 \longrightarrow \alpha + \gamma_{HC} \qquad (1)$$

The high carbon austenite then decomposes into bainitic ferrite plus carbide.

$$\text{Stage II:} \qquad \gamma_{HC} \longrightarrow \alpha + \text{carbides.} \qquad (2)$$

The desirable mechanical properties; toughness and ductility plus high strength, (which result from the bainitic ferrite/retained austenite microstructure), deteriorate quickly if stage II is allowed to occur. Therefore, the length of the austemper cycle is critical. For industrial applications the widest possible 'processing window' is desired.

Segregation of alloying elements can seriously impair the mechanical properties obtained in the austempering process. Unalloyed DI's usually contain about 3.5 wt. % C, 2.5 wt. % Si and 0.3-0.5 wt % Mn [3]. For the present work steel alloys were chosen to model DI's because of the metallographic difficulties produced by the graphite nodules. These nodules have a tendency to pull out or smear during polishing and grinding operations in the actual cast iron structure, making thinning difficult. These steels simulate the cast iron matrix, that is, a ductile cast iron structure without the graphite nodules, at austenitizing temperatures. This model also eliminates any variation in C content during austenitization, because the cast iron has an infinite source of C in the graphite nodules and any differences in the

austenitizing temperature would result in varying amounts of C in solution. The C and Si compositions were chosen to match the iron matrix composition of ductile cast irons austenitized at 850-900° C (C = 0.7%, Si = 2.5%). Manganese additions of 0.3 to 3.0% were studied because Mn is an important alloying element in most heat treatable steels and, although DI's will normally contain only 0.3% Mn, segregation may increase this level locally by a factor of ten. The 0.3% Mn alloy was used as a reference material because it has the same composition as the standard unalloyed DI and because retained austenite ($R\gamma$) data already existed for this alloy. By using up to 3% Mn the effects of microsegregation at the cell boundaries can be predicted. Simulating a highly segregated matrix will cause any effects due to high Mn content to be obvious when compared to the 0.3 Mn reference alloy. In ADI, the Mn content in the bainitic reactions is of great concern because Mn is a strong austenite stabilizer. High concentrations of Mn near the boundary of each cell (the midpoint region between graphite nodules) will create areas of untransformed austenite (γ_0) and/or martensite, thus reducing machinability and mechanical properties. Properly selected alloying elements and high nodule counts, resulting in smaller cells and a more homogeneous microstructure, are therefore critical in bainitic iron production.

This thesis presents the results of a number of experiments aimed at determining the effect of Mn on the length of the stage I reaction. A basic knowledge of the effects of Mn will yield a more complete understanding of the austempering process for the normal case and also when microsegregation is present. The onset time for stage II in

ductile irons is a critical parameter because of the associated degradation of the mechanical properties which result from carbide formation.

II. EXPERIMENTAL PROCEDURE

To determine stage II onset times as a function of manganese (Mn) content, four alloys containing Fe + 2.5 Si + 0.7 C + X, where X is 0.3, 1, 2, or 3 percent Mn were produced. Several casting methods were explored including drop casting, solidification in the crucible, and chill casting in an attempt to understand and reduce the porosity present in the samples. The final method chosen was a carefully controlled chill casting technique. The four alloy compositions were prepared by melting A101 Electrolytic grade iron (99.98%), spectroscopic grade C rods, semiconductor grade silicon, and 99.97% manganese in high purity Al_2O_3 crucibles. A 3 kHz power converter was used to ensure good mixing. Previous studies [4] have shown that mixing is adequate to produce a uniform carbon composition throughout an eight inch long ingot. Also, previous work [4] has shown that the use of a graphite cloth insulation around the crucible eliminates decarburization and assures final carbon compositions close to the target compositions. After induction melting, the steels were heated an additional 100 to 150° C and vacuum degassed for several minutes. After cooling slightly and backfilling with high purity argon, the melt was cast at about 1500° C.

Initially, each two inch diameter chill casting was austenitized and then furnace cooled to homogenize the carbon and sotten the billets. These cylindrical billets were then cut into 1 cm thick slices, sealed in a stainless steel jacket under a partial argon atmosphere to prevent decarburization, and hot rolled at 880° C to about 0.2 cm sheet. The

rolling temperature which was originally 700° C was increased to 880° C to help close the remaining porosity. The sheet was cut into 15 mm square samples thereby producing about a dozen samples from the original 1 cm slice. These samples were numbered consecutively.

The rolling produces a large BCC rolling texture in which the {100} planes prefer to lie parallel to the rolling plane [5]. The main analytical technique used to follow the austempering kinetics in this work was the measurement of retained austenite ($R\gamma$) by x-ray diffraction. Quantifying the $R\gamma$ by this method is more difficult when a preferred orientation is present. It is therefore desirable to remove this texture when possible.

Texture, or a preferred orientation, is often present in steels as a result of columnar solidification or plastic deformation. However, this texture can be essentially removed by austenitizing and then cooling the steel to produce a new set of grains [6]. Summary tables of some experiments demonstrating this fact are included in the Results section. Removal of the deformation texture was achieved in the following manner. The 15 mm x 15 mm samples cut from the rolled sheet were surface ground flat. Some difficulty in obtaining satisfactory $R\gamma$ data was encountered initially with the heat treating procedures which may have resulted in surface decarburization due to inadequate care in insuring that a low O_2 partial pressure existed during austenitization. The major cause of this difficulty was several small leaks in the vacuum lines. Following is a description of the improved procedure which was employed after the leaks were repaired resulting in about 1.5 orders of magnitude better vacuum. The samples were loaded into a vacuum system

attached to the furnace which was purged several times with helium and then connected to a diffusion pump which was allowed to pump overnight. The next day liquid nitrogen was added to the cold trap so that a vacuum level in the 10^{-7} torr range was established. At this point, the furnace was turned on. When the temperature of the samples reached roughly 400° C, the vacuum pumps were closed off and the system was backfilled with helium to slightly less than atmospheric pressure. The samples were then austenitized at 900° C for one hour and cooled to less than 300° C in the helium environment. This austenitization and cooling process was performed a second time. The samples were then prepared for x-ray analysis by surface grinding and electropolishing as described in more detail below.

A set of six different diffraction peaks were examined from a standard x-ray diffractometer two theta scan. According to theory [7], if the grains (of ferrite in this case) possess a random orientation then the area under each peak is predicted to be:

$$I(hkl)_\alpha = \frac{K\, R(hkl)}{\mu} X_\alpha \qquad (3)$$

where : $I(hkl)_\alpha$ = area under the body centered cubic (hkl) peak

K = a constant for given x-ray tube output intensity and beam diameter

μ = the linear absorption coefficient of the steel

X_α = volume fraction of the α phase

and $R(hkl)_\alpha$ is a function of the particular reflection:

$$R = F^2\, P\, LPF\, \exp(-2M)/\, v^2$$

where: F = structure factor

P = multiplicity

LPF = Lorentz Polarization Factor

exp(-2M) = Debye-Waller factor

v = volume of the unit cell

So that I/R = constant.

One can see then that the ratio of I/R is a constant for each peak in the spectra. A more detailed discussion of the terms in the above equations may be found in books on x-ray analysis [7] or papers on retained austenite measurements [8] [9].

When a preferred orientation exists the I/R ratio will be larger than for a specimen with a completely random orientation of grains. A qualitative texture parameter has been defined by Dickson [10] using the above ideas as:

$$P(hkl)_\alpha = \frac{[I/R](hkl)_\alpha}{1/n \sum_{i=1}^{n} [I/R](hkl)_\alpha (i)} \qquad (4)$$

where n is the number of different peaks in the diffraction pattern. If $P(hkl)_\alpha = 1$ there is no texture; if $P(hkl)_\alpha > 1$, the $(hkl)_\alpha$ planes are most likely to lie parallel to the surface; if $P(hkl)_\alpha < 1$, the $(hkl)_\alpha$ planes have a preferred orientation away from the surface. In the present work the area under the six α peaks was measured and $P(hkl)_\alpha$ was calculated for each. The standard deviation (σ_p) of these six values was determined and used to quantify the texture present. Results from

this work confirm earlier experiments [6] showing that σ_p is about 0.6 in the as-rolled condition, whereas a random sample can be characterized within experimental accuracy by a value of $\sigma_p \lesssim 0.1$. The ideal case, a completely random orientation, would be given by a value of $\sigma_p = 0$. After this procedure was established for adequately removing texture, the main task of measuring the $R\gamma$ formed during austempering was performed.

Samples ground flat after rolling were cycled across the A_3 line twice under the moderate vacuum conditions described above. This reduced the rolling texture to an acceptable level ($\sigma \lesssim 0.1$) through phase transformations. As the first step in the austempering process, the samples were then austenitized again for one hour without removing them from the helium atmosphere. At this point they were removed from the vacuum system and quickly quenched into a salt bath held at 370° C. The transformation of γ to α, γ_{HC}, and carbides was then allowed to occur for times ranging from three minutes to three weeks. These reactions were terminated by a water quench. A number of experiments were conducted using various combinations and amounts of hand polishing, surface grinding, and electropolishing to establish a surface treatment prior to x-ray analysis. The purpose of this process was to yield reproducible measurements by removing any decarburization layer without 1) introducing a deformation texture during grinding and 2) transforming any of the $R\gamma$ produced during austempering. The procedure which gave the most consistent results was as follows: remove 10 mils by surface grinding and then electropolish for three minutes in a 6% perchloric acid, 35% 2-butoxy-ethanol, and 59% methanol solution at 0° C. This

polishing procedure is a slight modification of a more common electropolishing technique normally done at -70° C using only methanol and perchloric acid. For this work 35% of the methanol was replaced with 2-butoxy-ethanol and the polishing was carried out at 0° C. The reason this 0° C procedure was used was to prevent transformation of any of the $R\gamma$ formed during austempering to martensite by not quenching the γ to as low a temperature.

A diffraction scan was then obtained as described above. Four austenite peaks, the {111}, {200}, {220}, and {311}, and four ferrite peaks, the {110}, {200}, {211}, and {220} were examined. Using arguments similar to those used in the development of the texture equation (4), one can determine the volume fraction of a given phase from this diffraction pattern.

For randomly oriented grains in a substance containing more than one phase the area under each diffraction peak is given by theory [7] as noted earlier in equation (3) as:

$$I(hkl)_1 = \frac{K\, R(hkl)_1}{\mu_{mix}} X_1 \qquad (3)$$

where μ_{mix} is the linear absorption coefficient for a mixture of the phases, X_1 is the volume fraction of phase 1, and R and K are constants.

If only two phases are present, the sum of the two volume fractions must be equal to unity or:

$$X_1 + X_2 = 1 \qquad (5)$$

Then equation (3) can be applied to each phase, ferrite and austenite in this case, and a ratio of the intensities formed:

$$\frac{I_1}{I_2} = \frac{R(hkl)_1}{R(hkl)_2}\frac{X_1}{X_2} \qquad (6)$$

Combining equations (5) and (6) produces an expression for the amount of retained austenite in terms of the (I/R) ratios for the ferrite (α) and austenite (γ) phases:

$$X_\gamma = \frac{1}{1+[(I/R)_\alpha / (I/R)_\gamma]} \qquad (7)$$

For greater accuracy, or in the case where some preferred orientation exists, the use of more than one diffraction peak is necessary, and equation (7) then becomes:

$$X_\gamma = \frac{1}{1+[(1/n)\sum_{i=1}^{n}(I/R)_\alpha \; / \; (1/m)\sum_{i=1}^{m}(I/R)_\gamma]} \qquad (8)$$

It is now clear why knowing when a preferred orientation exists is important in determining the amount of $R\gamma$. If the I/R ratio is larger or smaller than theory predicts for an individual reflection, the calculated value of X_γ will not be a true measure of the fraction of γ present.

A plot of % $R\gamma$ versus austempering time reveals the two stage nature of the γ to bainitic ferrite transformation. The % $R\gamma$ rises quickly at first and then flattens out. After some time the amount of $R\gamma$ begins to decrease rapidly indicating the onset of the stage II reaction. This forms a plateau shape. Plotting Rockwell hardness (R_c)

versus austempering time also shows the two stages (see for example the plots in Figure 5).

The microstructures observed in an optical microscope during the initial rise in % $R\gamma$ are: martensite + $R\gamma$ + a small amount of bainitic ferrite. On the flat portion of the plateau only $R\gamma$ and bainitic ferrite are present. Finally as the % $R\gamma$ drops again, $R\gamma$ and an increased amount of bainitic ferrite are observed. The carbides (believed to be ε carbides), which form during this drop in $R\gamma$, are not large enough to be seen optically.

III. EXPERIMENTAL RESULTS

A. Texture Experiments

Table 1 summarizes the chemical concentrations, as measured by the analytical services group at the Ames Laboratory US DOE, for the alloy compositions studied. Table 1 also gives a key to sample naming conventions.

After collecting the x-ray scan, the data were analyzed by an interactive Fortran graphics program. The texture analysis program, which automatically subtracts background and calculates area under the peaks, has an option for manual manipulation of the background for each peak by the programmer.

Although data were collected for the {111} γ and {110} α peaks, these peaks were not included when calculating σ_p or % $R\gamma$ for any of the data given in this thesis. The reason they were excluded is because the two peaks were not well enough resolved to give good results in all cases. In Table 2, the first set of data demonstrates the large preferred orientation present as a consequence of the rolling operation. Values of σ_p larger than 0.1 indicate significant amounts of texture present. The second set of data shows the condition of samples after the rolling texture has been removed by cycling across the A_3 line twice, as described in the Experimental Procedures section. These results represent an attempt to quantify the effects of combinations of hand polishing, surface grinding, and varying amounts of

Table 1. Chemical analysis of alloys in weight percent and sample naming conventions

	Measured Compositions			Target Compositions		
Alloy designation	%C	%Si	%Mn	%C	%Si	%Mn
KHA	.676	2.475	0.291	0.7	2.5	0.3
KHB	.709	2.454	1.00	0.7	2.5	1.0
KHC	.651	2.479	1.99	0.7	2.5	2.0
KHD	.726	2.441	3.04	0.7	2.5	3.0
KH2C	.782	NA	NA	0.78	2.5	2.0
KH2D	.728	NA	NA	0.78	2.5	3.0
KHDF	.778	2.535	0.289	0.9	2.55	0.3

NA = Not analyzed.

The sample naming convention used was as follows: KH(alloy)(sample #)_(time at the austempering temperature in hours)(condition of sample), where the alloy is described by a letter A-D. The condition of the sample is delineated by the following:

A or B	one half of what used to be one large sample
sg	surface ground
hp	hand polished
EP	electropolished
e#	EP for # seconds
a#	R_γ file in the as EP condition unless noted
at#	texture file after austempering EP condition unless noted
x#	x-ray again sample w/o any changes in surface condition
R	rotate the sample 90° and x-ray again
c	chemically etched
h	heat treated for texture removal
H	held at 1100° C for 5 days to homogenize Si and Mn

Table 2. Results of texture experiments

set 1

ALLOY KHDF (Fe + 2.475 Si + .676 C + .291 Mn)

Sample	Texture (σ_p)	Condition/Comments
DF1	0.485	Rolled and EP
DF2	0.598	" " "
DF6	0.434	" " "
DF7	0.560	" " "
DF8	0.637	" " "
DF9	0.485	" " "
DF1h	0.081	texture removed but not EP
DF1h	0.050	" " and EP
DF2h	0.119	" " but not EP
DF2h	0.090	" " and EP

set 2 ALLOY KHA (Fe + 2.475 Si + .676 C + .291 Mn)

Sample	Texture (σ_p)	Condition/Comments
12sg	.062	surface ground
12e90	.093	electropolish (EP) 90 sec
12e150	.119	EP 150 sec
11e120	.070	EP 120 sec
2e	.074	EP
3e	.096	EP
3hp	.094	hand polished (HP)
4hp	.066	" "
20hp	.095	" "
10hp	.080	" "
10hpx	.080	x-ray the above sample again
10e30	.064	EP and x-ray again
6sg	.080	surface grind(SG) and x-ray
8sg	.066	" " " "
8sgx	.056	simply x-ray again
7sg	.069	SG and x-ray
19sg	.046	" " "
5hp	.088	HP
5hpx	.108	x-ray again
5hpx2	.082	" "
5hpx3	.110	" "
5e30	.097	EP 30 sec and x-ray
5e60	.100	EP 60 sec " "
8sge30	.075	EP 30 sec " "

electropolishing on the preferred orientation. For a given sample and condition, the texture can be measured to $\pm$ 0.02 in σ_p. Note, for example, sample 5 for which σ_p was measured four times varying between 0.082 and 0.110. Verhoeven and Downing [6] have shown that a significant texture can result from hand polishing. However, the magnitude of texture induced in a sample when hand polished by different people is much more random. Thus, there appear to be a number of factors involved in determining the extent of this texture, the human operator probably being the most significant. It was not the purpose of this work to quantify deformation induced texture, however, these facts were of concern because a texture free sample was the desired starting point for $R\gamma$ studies. This second set of data therefore is included to demonstrate adequate and reproducible texture removal with the procedures used. In almost all cases σ_p is reduced from around 0.5 or greater to less than 0.1.

B. Retained Austenite Experiments

A second Fortran program, called AUS, was used for the retained austenite analysis. AUS also allowed interactive correction of the background subtraction from the x-ray scan. Texture was again calculated by AUS as a check on the validity of the $R\gamma$ data. A sample output from AUS is included in Figures 1a-c, which show a plot of the two theta scan and the results from both the automatic and manual modes for calculating $R\gamma$.

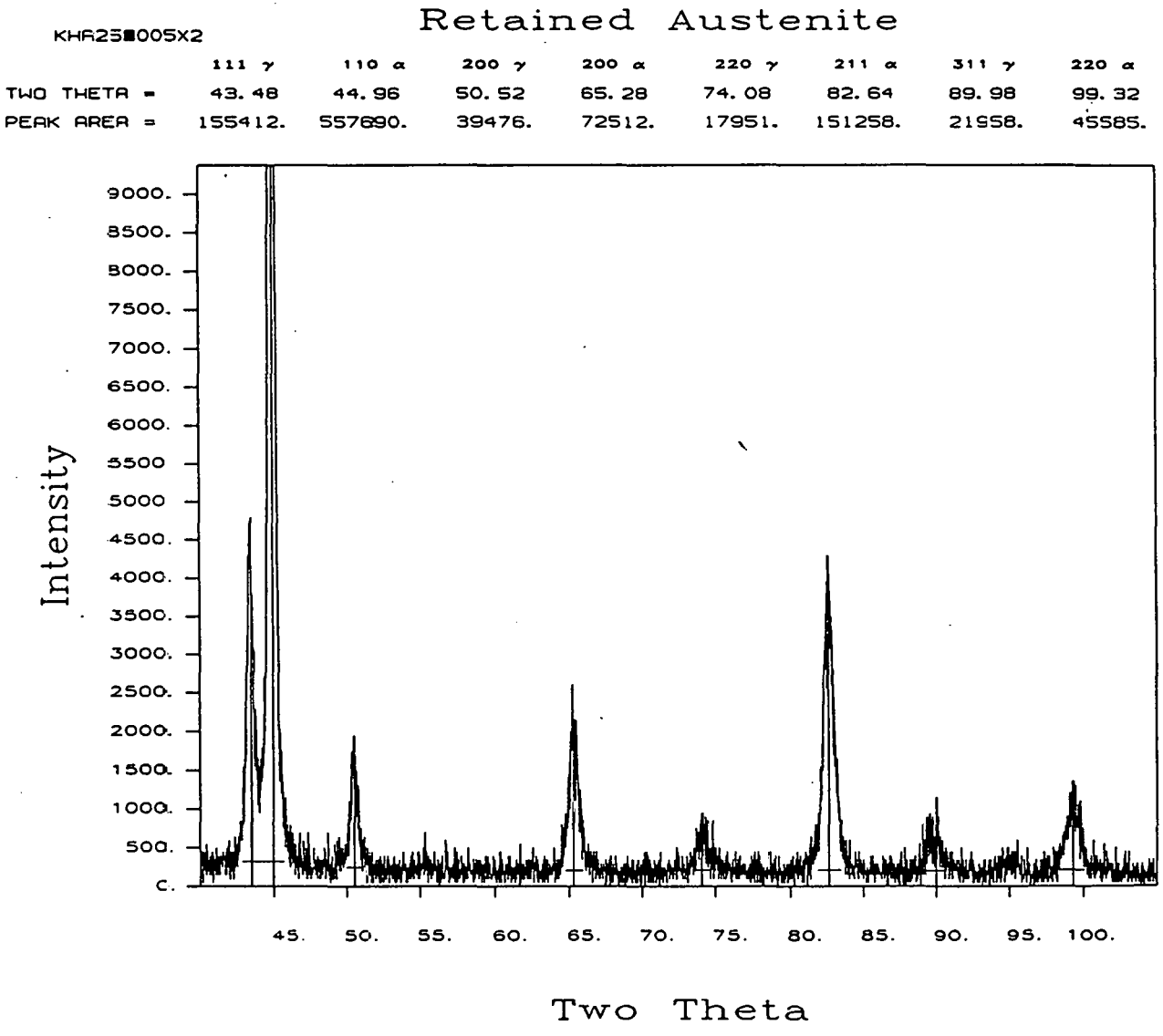

Figure 1a. Sample output plot of a two theta scan from AUS

DATA SET = KHA25_005X2 AUTO

START	CENTER	END	INT	A	A1	R	FF	LP	DW	I/R	2TH	F
4218	4348	4402	165756.0	3.6019	3.6019	242.457	5777.610	11.955	0.958	683.6514	43.48	18.703
4404	4496	4600	540778.0	2.8486	2.8486	334.306	1405.074	11.087	0.955	1617.6134	44.96	18.442
4906	5052	5190	50860.0	3.6129	3.6095	109.841	5066.001	8.506	0.945	463.0313	50.53	17.494
6312	6528	6696	90703.0	2.8578	2.8563	46.530	966.471	4.786	0.913	1949.3370	65.28	15.244
7162	7408	7546	32717.0	3.6130	3.6159	59.140	3313.234	3.705	0.893	553.2144	74.09	14.090
7960	8264	8424	177489.0	2.8582	2.8571	85.665	719.130	3.100	0.873	2071.8914	82.64	13.108
8810	8998	9276	31594.0	3.6127	3.6137	67.063	2568.895	2.826	0.856	471.1078	89.99	12.371
9708	9932	10250	61938.0	2.8588	2.8579	28.219	563.759	2.729	0.834	2194.9045	99.32	11.572

FCC A_AVG = 3.6101 (0.0055) ABCC A_AVG = 2.8558 (0.0049) AFCC A1_AVG = 3.6102 ABCC A1_AVG = 2.8550

	P(111G)	P(200G)	P(220G)	P(311G)	G-STD-DEV	P(110F)	P(200F)	P(211F)	P(220F)	F-STD-DEV
ALL PEAKS	1.260	0.853	1.019	0.868	0.308	0.826	0.995	1.058	1.121	0.196
ALL PEAKS	0.000	0.934	1.116	0.950	0.138	0.000	0.941	1.000	1.059	0.073

	ALL	468	246	248	268	24	26	28	46	48	68	2	4	6	8
ALL	21.70	20.76	22.41	21.67	22.03	23.33	22.73	22.16	21.26	20.76	20.28	25.12	21.78	20.76	19.83
3+5+7	20.20	19.31	20.87	20.18	20.52	21.75	21.18	20.64	19.78	19.31	18.86	23.46	20.28	19.31	18.43
1+5+7	22.52	21.55	23.25	22.50	22.86	24.20	23.58	23.00	22.07	21.55	21.06	26.03	22.60	21.56	20.60
1+3+5	22.44	21.47	23.16	22.41	22.78	24.11	23.50	22.91	21.99	21.47	20.99	25.94	22.52	21.48	20.52
1+3+7	21.59	20.65	22.29	21.56	21.92	23.22	22.62	22.05	21.15	20.65	20.18	25.00	21.67	20.65	19.72
1+3	22.65	21.67	23.37	22.62	22.99	24.33	23.71	23.12	22.19	21.67	21.18	26.17	22.73	21.67	20.71
1+5	24.00	22.99	24.76	23.97	24.36	25.75	25.11	24.50	23.52	22.99	22.47	27.66	24.08	22.99	21.98
1+7	22.77	21.79	23.50	22.74	23.11	24.46	23.84	23.25	22.31	21.79	21.30	26.30	22.85	21.79	20.83
3+5	20.60	19.69	21.28	20.58	20.92	22.17	21.60	21.05	20.17	19.69	19.24	23.90	20.68	19.69	18.80
3+7	19.26	18.39	19.90	19.23	19.56	20.75	20.20	19.68	18.85	18.39	17.96	22.40	19.33	18.40	17.55
5+7	19.26	18.39	19.90	19.23	19.56	20.75	20.20	19.68	18.85	18.39	17.96	22.40	19.33	18.40	17.55
1	25.88	24.81	26.67	25.85	26.25	27.71	27.04	26.40	25.37	24.81	24.27	29.71	25.96	24.81	23.75
3	19.12	18.26	19.77	19.10	19.43	20.61	20.06	19.54	18.72	18.26	17.83	22.25	19.19	18.27	17.42
5	22.03	21.07	22.74	22.00	22.36	23.68	23.07	22.49	21.58	21.07	20.59	25.48	22.11	21.07	20.13
7	19.39	18.52	20.04	19.37	19.70	20.90	20.34	19.82	18.98	18.52	18.09	22.55	19.46	18.53	17.67

Figure 1b. Sample output of Rγ calculations using the auto mode of AUS

DATA SET = KHA25_005X2 MANUAL

START	CENTER	END	INT	A	A1	R	FF	LP	DW	I/R	2TH	F
4282	4348	4402	155412.0	3.6019	3.6019	242.457	5777.610	11.955	0.958	640.9883	43.48	18.703
4404	4496	4570	557690.4	2.8486	2.8486	334.306	1405.074	11.087	0.955	1668.2030	44.96	18.442
4996	5052	5094	39476.0	3.6129	3.6095	109.841	5066.001	8.506	0.945	359.3910	50.53	17.494
6472	652E	6594	72511.9	2.8578	2.8563	46.530	966.471	4.786	0.913	1558.3834	65.28	15.244
7370	740E	7466	17950.9	3.6130	3.6159	59.140	3313.234	3.705	0.893	303.5338	74.09	14.090
8190	8264	8344	151257.7	2.8582	2.8571	85.665	719.130	3.100	0.873	1765.6844	82.64	13.108
8914	8998	9060	21957.7	3.6127	3.6137	67.063	2568.895	2.826	0.856	327.4180	89.99	12.371
9838	9932	10008	45585.4	2.8588	2.8579	28.219	563.759	2.729	0.834	1615.4143	99.32	11.572

FCC A_AVG = 3.6101 (0.0055) ABCC A_AVG = 2.8558 (0.0049) AFCC A1_AVG = 3.6102 ABCC A1_AVG = 2.8550

	P(111G)	P(200G)	P(220G)	P(311G)	G-STD-DEV	P(110F)	P(200F)	P(211F)	P(220F)	F-STD-DEV
ALL PEAKS	1.572	0.881	0.744	0.803	0.648	1.010	0.943	1.069	0.978	0.091
ALL PEAKS	0.000	1.089	0.919	0.992	0.120	0.000	0.946	1.072	0.981	0.091

	ALL	468	246	248	268	24	26	28	46	48	68	2	4	6	8
ALL	19.80	19.85	19.68	19.50	20.17	20.18	19.19	19.90	19.70	20.45	19.44	19.64	20.74	18.76	20.16
3+5+7	16.66	16.70	16.55	16.40	16.98	16.99	16.13	16.74	16.57	17.22	16.34	16.52	17.48	15.75	16.97
1+5+7	20.42	20.48	20.30	20.12	20.80	20.81	19.80	20.52	20.32	21.08	20.05	20.26	21.39	19.36	20.79
1+3+5	20.83	20.88	20.71	20.52	21.22	21.22	20.20	20.93	20.73	21.50	20.45	20.67	21.81	19.75	21.20
1+3+7	21.13	21.19	21.01	20.82	21.52	21.53	20.50	21.23	21.03	21.81	20.75	20.97	22.12	20.04	21.51
1+3	23.24	23.30	23.11	22.91	23.66	23.67	22.56	23.35	23.13	23.97	22.83	23.07	24.30	22.07	23.64
1+5	22.23	22.29	22.11	21.91	22.64	22.64	21.57	22.34	22.13	22.93	21.84	22.06	23.26	21.10	22.62
1+7	22.67	22.73	22.54	22.34	23.08	23.08	22.00	22.78	22.56	23.38	22.26	22.50	23.71	21.52	23.06
3+5	16.71	16.76	16.61	16.45	17.04	17.04	16.18	16.80	16.63	17.28	16.39	16.58	17.54	15.81	17.03
3+7	17.21	17.26	17.11	16.95	17.54	17.55	16.67	17.30	17.12	17.79	16.88	17.07	18.06	16.28	17.53
5+7	17.21	17.26	17.11	16.95	17.54	17.55	16.67	17.30	17.12	17.79	16.88	17.07	18.06	16.28	17.53
1	27.96	28.02	27.81	27.58	28.43	28.43	27.18	28.08	27.83	28.77	27.49	27.76	29.14	26.63	28.41
3	17.87	17.92	17.76	17.60	18.21	18.22	17.31	17.96	17.78	18.47	17.53	17.72	18.74	16.91	18.20
5	15.52	15.57	15.43	15.28	15.83	15.84	15.02	15.60	15.44	16.06	15.22	15.39	16.30	14.67	15.82
7	16.54	16.59	16.44	16.29	16.86	16.87	16.02	16.63	16.46	17.10	16.23	16.41	17.36	15.64	16.85

Figure 1c. Sample output of R_γ calculations using the manual mode of AUS

In all of the retained austenite experiments the austempering quench was to 370° C. The first R_γ experiment listed in Table 3 used four samples of alloy KHA (0.3% Mn), all austempered for one half hour at 370° C. The R_γ values were much lower than expected and also showed a large variation. Before beginning work on the Mn alloys, KHDF, an alloy similar to alloy KHA was used to check our experimental setup and procedures. It was possible to reproduce accurately previous work [11] using this alloy. A second, identical experiment was therefore performed with a few samples of alloy KHDF included for control purposes. The results (see Table 3 set 2) for KHA were again poor, i.e., low and scattered (between 4% and 16% R_γ). R_γ values for KHDF were around 27%, as expected from our earlier work and that of another researcher [11].

Three experiments were then performed on alloy KHB (see Table 4), with careful attention being paid to starting sample thickness. In the first experiment (Table 4 set 1) the R_γ values were again low and varied greatly. It was observed that in set 1 the starting sample thicknesses were not all the same. Therefore, in set 2, four new samples were surface ground to the same starting thickness (1.52 mm) and austempered. This second experiment (Table 4 set 2) seemed to confirm that uniform sample thickness was necessary for consistent R_γ results. However, when samples from each of the first two experiments were included in the third experiment (Table 4 set 3) in an effort to reproduce these results, none of the measured R_γ values matched the previous data. For example sample 6 used in set 1 dropped from ~ 27% to 16%, sample 9 of set 1 from 14 to 6%, sample 7 of set 2 from 29 to 18%, etc.

Table 3. Results of Retained Austenite experiments using 0.3% Mn alloy

ALLOY KHA (Fe + 2.475 Si + .676 C + .291 Mn)

Sample	Texture (σ_p)	Vol. % R.A.	Condition/Comments
set 1			
5a		14.01	
5at	.062		
7a		18.83	
7at	.064		
7ae		18.18	
8a		12.49	
8at	.049		
8ae		12.58	
20a		14.24	
20at	.087		
20ehpe		15.57	HP 20a EP again
set 2			
4a		16.41	
6a		15.25	
6ax2		15.15	repeat 6a above
6at	.059		
6atx2	.037		repeat 6at above
19a		4.08	
19at	.092		
19ax2		9.32	SG and x-ray again
10a		9.51	
KHDF1		27.14	
KHDF8		24.52	
KHDF8AT	.059		

Table 4. Results of Retained Austenite experiments using 1.0% Mn alloy

ALLOY KHB (Fe + 2.454 Si + .709 C + 1.00 Mn)

Sample	Texture (σ_p)	Vol. % R.A.	Condition/Comments
set 1			
Before austempering			
6x2	0.051		
9	0.095		SG and not EP
10	0.104		SG and not EP
3	0.071		SG and not EP
after austempering w/o SG only EP as noted			
6a		18.85	not EP
6at	0.051		not EP
6a		25.25	EP
10a		0.89	not EP
10a		0.24	EP
10ax2		0.59	HP and EP again
9a		1.05	
5a		13.10	
at this point surface grind all 4 samples EP and x-ray			
6asg		27.14	
6ax2		27.38	
6aR		28.15	rotate 90° and x-ray
10ax2		3.22	
9a		3.14	
5ax2		17.87	
SG again at this point EP and x-ray (only 9 and 10)			
9ax2		14.41	
10ax3		17.13	
set 2 (Surface ground 4 new samples to same thickness and austemper)			
3a		29.87	
1a		29.58	
1ax2		29.36	
1atx2	0.020		
1ax3		29.53	
7a		30.25	
7ax2		29.16	
8a		28.88	
8ax2		28.85	
8ax3R		27.80	
4a		30.60	
4at	0.093		

Table 4. Continued

Sample	Texture (σ_p)	Vol. % R.A.	Condition/Comments
set 3 (repeat experiment, i.e., austenitize and austemper again with samples 5,6,7,9,10)			
10a2		14.16	
9a2		6.33	
9a2x2		6.60	
9a2c		7.23	HHB chemically etch
9a2c2		9.17	with $HF/H_2O_2/H_2O$
9a2R		9.76	rotate 90°
5a2		11.64	
5a2x2side		8.28	x-ray off to one side
6a2		16.24	
7a2		18.00	

At this stage it was thought that these inconsistencies were a result of the amount of surface removed. After austempering four KHC samples and again obtaining low values for $R\gamma$ (see Table 5), 15 mils were removed (by surface grinding) from two of the samples, after which the $R\gamma$ rose to the anticipated value. Material was then removed incrementally, followed by analysis after each increment, for the two remaining samples; after a total of 8 mils was removed, the $R\gamma$ had again increased into the expected range. A plot of surface removed versus $R\gamma$ is given in Figure 2. These results indicate that a decarburization effect may have been responsible for the scatter in the data.

Using everything that was learned so far, the next experiment was performed after the improvements in the vacuum level described in the the Experimental Procedure section were made. The reason these improvements were needed was to lower the O_2 content in the experimental atmosphere and reduce the decarburization. The magnitude of the $R\gamma$ measured in the next experiment (see Table 5 set 2) was as predicted, but the scatter, although considerably lower than before, was still puzzling as these samples were identical. A check of the Rockwell C (R_c) hardness for selected samples from these experiments showed that those with lower $R\gamma$ content (around 25%) had high R_c (around 55), while the samples with $R\gamma \simeq 31\%$ had $R_c \simeq 48$. It was thus apparent that the 2% Mn alloy had not yet reached a maximum in $R\gamma$ after 30 minutes of tempering at 370° C, but still contained some martensite.

So far all measurements were made after austempering for 30 minutes, which was estimated to be a point of maximum $R\gamma$ content based on previous experience with a 0.3% Mn alloy. This proved not to be the

Table 5. Results of Retained Austenite experiments using 2.0% Mn alloy

ALLOY KHC (Fe + 2.479 Si + 0.651 C + 1.99 Mn)

Sample	Texture (σ_p)	Vol. % R.A.	Condition/Comments
5a		3.28	Directly from salt bath
5at	0.059		" " " "
9a		2.71	" " " "
8a		5.82	" " " "
Now HP and x-ray w/o EP			
9ahp		6.69	
5ahp		6.35	
5athp	0.151		
8ahp		13.99	
EP and x-ray			
5ae120		8.00	
5ate120	0.094		
8ae120		17.38	
SG ~ 15 mils and EP			
8a2		28.98	
5a2x2		29.70	
5at2	0.092		
SG 4 mil off #7 and 3 mils off #9			
7a		14.69	
9a		11.25	
SG an additional 2 mils			
7a2		25.51	
7a2x2		25.43	
9a2		18.68	
9a2x2		18.68	
SG an additional 2 mils			
7a3		30.46	
9a3		27.06	
SG an additional 2 mils (total of 10 mils now)			
7a4		31.30	
9a4		29.44	
9a4x2		28.87	
SG an additional 2 mils			
7a5		32.31	
9a5		30.40	

Table 5. Continued

Sample	Texture (σ_p)	Vol. % R.A.	Condition/Comments
SG an additional 2 mils			
7a6		30.11	
7a6x2		30.44	
7a6x4		29.69	
7a6x5		29.78	
7a6x6		29.76	
9a6		29.88	
set 2			
2ax2		26.42	
3ax2		26.15	
4a		28.59	
4ax2		27.53	
4ax3		27.94	
4ax4		28.57	
6a		25.15	
6at	0.10		
6ax2		24.96	
6x3	0.116	25.34	
10a		28.04	
1a		25.31	
set 3 (next experiment)			
11a		31.67	
11ax2		31.57	
11ax3		31.66	
12ax2		30.61	
12ax3		30.52	
12at	0.145		
12atx2	0.153		
13ax2		30.34	
14ax2		30.21	
14ax3		30.41	
14ax4		30.72	
15ax2		33.71	
15ax3		33.16	
15atx2	0.101		
16ax2		34.62	
16ax3		34.22	
16atx2	0.118		

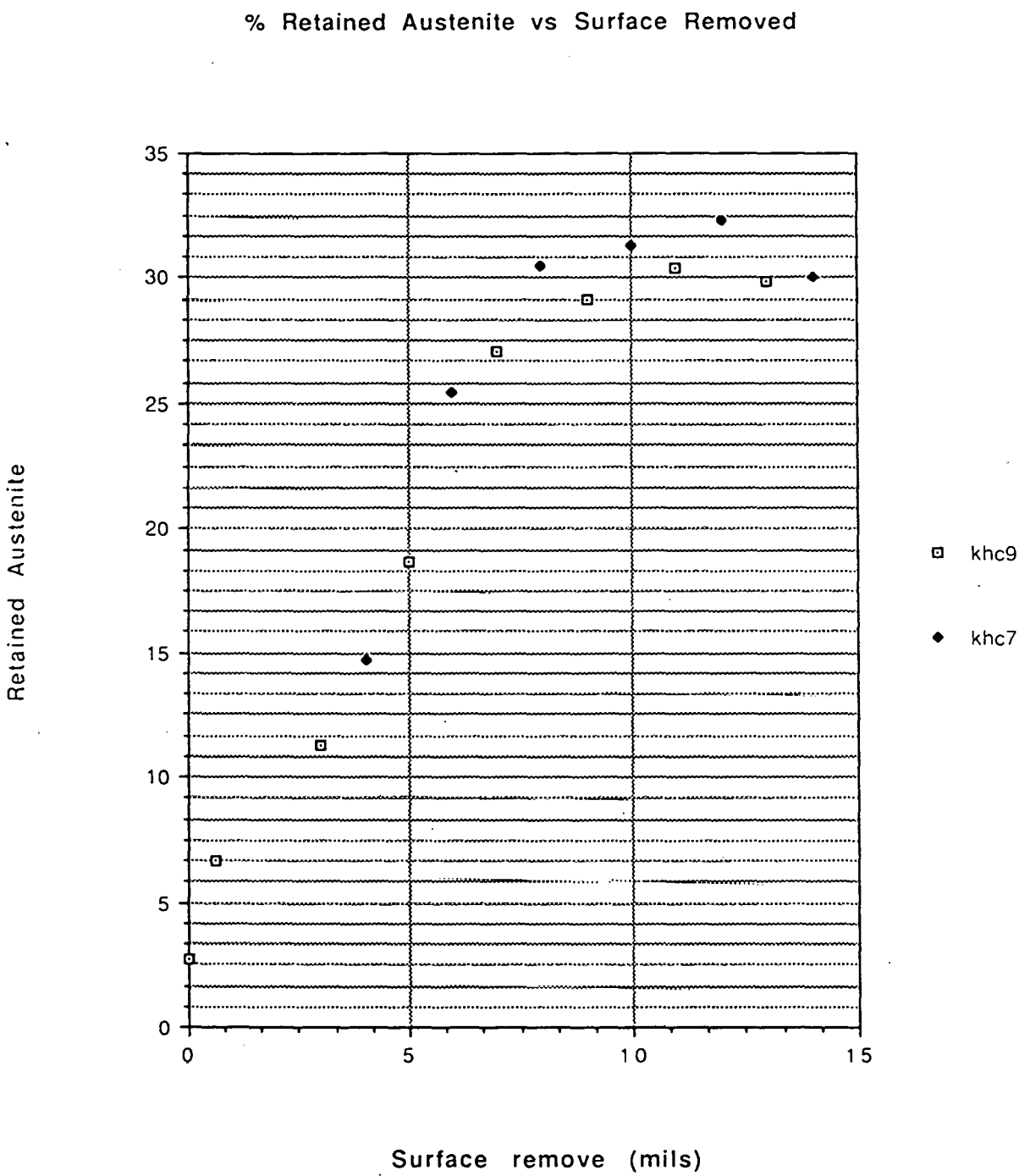

Figure 2. % $R\gamma$ versus surface removed for samples KHC7 and KHC9

case for alloys with Mn > 1.0%. $R\gamma$ measurements were made at this point for all four alloys as a function of austempering time. All of these measurements were completed using the following procedure. Austenitize the samples in an atmosphere with the lowest possible O_2 content. After austempering, the samples were prepared for x-ray analysis by removing 10 mils, 1/2 mil per pass, on an automated surface grinder with no coolant and then electropolishing for 3 minutes. Each alloy will be discussed separately and in detail followed by some more general observations in the next section.

Table 6 contains $R\gamma$ and R_c values for 5 sets of KHA data. These data are also displayed graphically in Figure 3. The first two sets represent an attempt to map the stage II reaction as a function of time. Note in sets 3 and 4, as with the KHA data presented earlier, the $R\gamma$ is much lower than expected from previous work using alloy KHDF. Also missing is a slow rise in the $R\gamma$ at short austempering times. These unexpected results are also present in the 1% and 3% Mn alloys. It is believed that the lower C content is responsible for these differences. In set 4, samples KHA46-48 are from a second ingot of the 0.3% Mn alloy. Chemical analysis of this ingot was completed for %C because the $R\gamma$ values were higher than expected. Near the top of the ingot the C was 0.669% and at the bottom the C measured 0.663%. Since this is the same C level as in the first ingot it is not known why the $R\gamma$ values are somewhat higher for these three samples. One possible explanation is that there may have been more segregation of Mn and Si than there was in the first 0.3% Mn ingot. Three data points from alloy KHDF are also plotted to show the level of $R\gamma$ initially expected. The fifth data set

Table 6. Results of Retained Austenite experiments using 0.3% Mn alloy as a function of time plus R_c results

ALLOY KHA (Fe + 2.475 Si + .676 C + .291 Mn)

Sample	Vol. % R.A.	R_c	Condition/Comments R_γ after SG 5 mils & x-ray
set 1			
22_05	13.9	42.3± 1.3	
23_10	6.6	41.3± 1.7	8.3
24_015	17.4	42.6± 1.8	17.6
25_005	18.5	43.4± 1.0	17.1
26_5	9.8	43.3± 0.5	10.2
27_8	9.1	43.7± 1.1	7.7
28_48	3.6	41.1± 1.6	
29_18	3.6	41.2± 1.5	
30_24	2.7	41.8± 2.0	
set 2			
31_005	18.9	43.6± 2.2	
32_015	17.8	41.8± 1.4	
33_05	14.4	42.3± 0.8	
34_5	8.9	----	
34Ē_5	9.1	39.8± 1.1	EP 10 min - no effect
35_10	6.1	42.0± 2.7	
36_8	9.0	42.8± 1.7	
37_18	2.3	39.2± 2.5	
38_24	2.3	40.8± 1.4	
39_70	2.8	40.7± 2.6	
set 3			
41_05	15.9	---	HP > 2 mils EP 10 min
41Ē_05	16.2	42.4± 1.1	EP 20 min total
KHDF̄3A_05	27.2	41.6± 1.4	
40_5	10.3	40.7± 1.1	
KHD̄F3B_5	23.3	42.5± 0.7	
set 4			
46_015	24.3	44.3± 1.0	
47_05	20.8	44.6± 0.4	
48_4	14.2	41.9± 3.2	
KHD̄F11_4	26.2	43.4± 0.4	
set 5			
48H_4	11.8	39.0± 2.8	Si and Mn Homogenized
40H_4	13.5	41.4± 0.7	" " " "

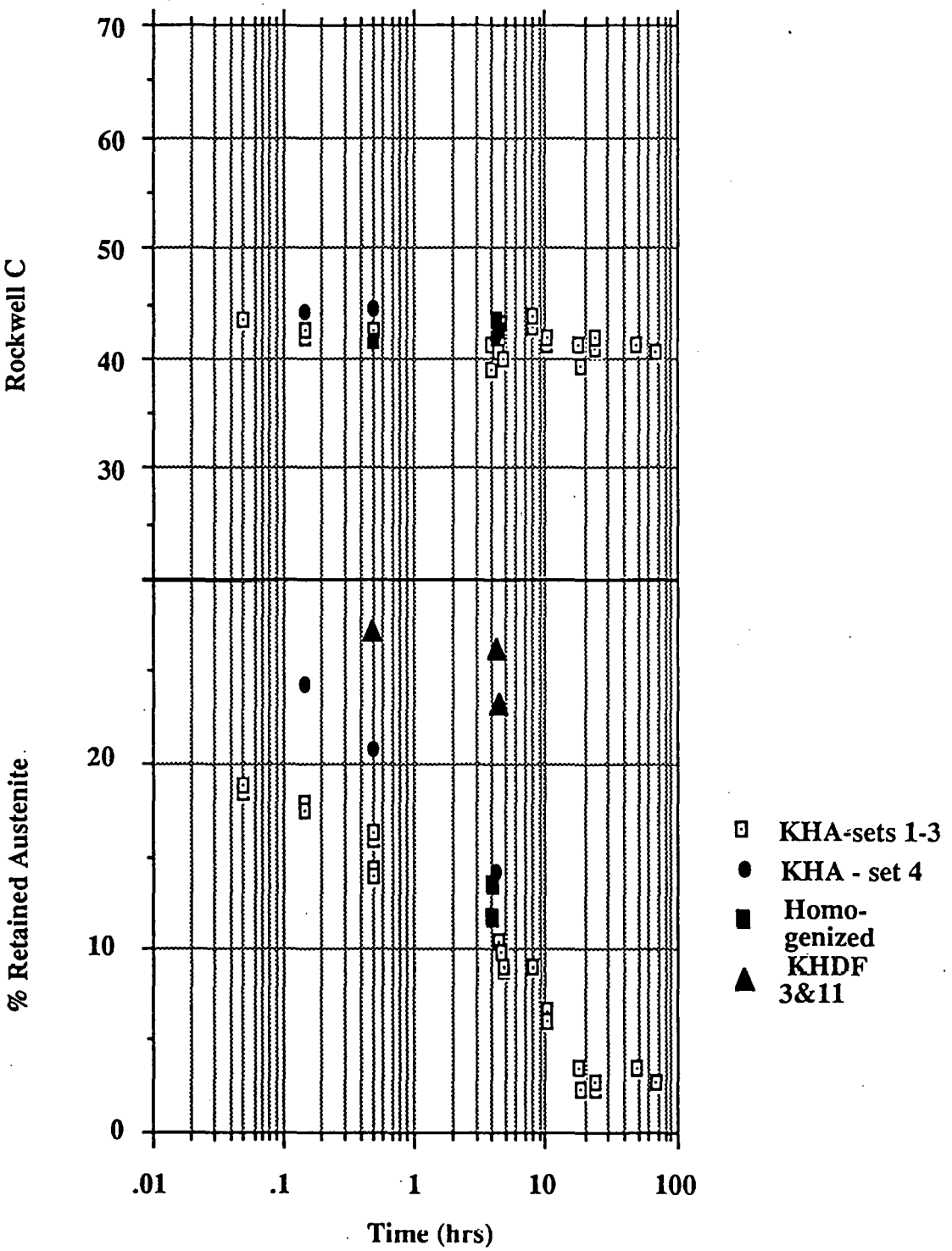

Figure 3. % R_γ and R_C versus time for the 0.3% Mn alloy KHA

is a portion of an experiment in which two samples from each alloy were heat treated at 1100° C for 5 days to homogenize the Si and Mn. The data for the other alloys in this homogenization experiment are included at the end of the appropriate table. The R_γ values changed little from the nonhomogenized samples, indicating that Si and Mn segregation did not contribute to the unexpected results mentioned previously.

Data for KHB in Table 7 and Figure 4 include R_γ and R_c as a function of austempering time. The results are again similar to KHA, that is, a low level of R_γ and only the right half of the plateau shape which is normally observed when plotting % R_γ versus austempering time.

KHC (Table 8 and Figure 5) is perhaps the most interesting alloy because the R_γ level exceeds 50%. KH2C (Table 9 and Figure 5) was produced to increase the carbon level from the 0.65% in KHC to ~ 0.78%, the same as in alloy KHDF. However, the high alloy content (Si + Mn) appears to have cancelled the effect of C so that the amount of R_γ was only slightly greater than for KHC. The entire plateau is also observed for R_γ , and the R_c data are as expected with respect to shape. The significant retarding effect of Mn on the rate of the stage I reaction (formation of bainitic ferrite) is quite obvious in this alloy, as stage II occurs only after almost two days of tempering.

For KHD (Table 10 and Figure 6) the lower R_γ level and lack of a plateau are again evident. KH2D (Table 11 and Figure 6) was also produced to increase the carbon level to ~ 0.78%, the same as in alloy KHDF. That goal was not reached as the resulting C was only 0.73%, the same as it was in the original KHD. For these 3.0% Mn alloys the R_c data shows that stage I occurs only to a small degree, even after three

Table 7. Results of Retained Austenite experiments using 1.0% Mn alloy as a function of time plus R_c results

ALLOY KHB (Fe + 2.454 Si + .709 C + 1.00 Mn)

Sample	Vol. % R.A.	R_c	Condition/Comments
15_015	24.37	44.0± 0.3	
20_03	25.3	41.0± 1.4	
13_1	21.5	40.2± 1.5	
16_5	19.1	---	
16E_5	21.9	39.8± 1.6	EP 10 min no effect
12_10	18.2	40.7± 1.2	
14_21	13.4	42.9± 0.6	
17_30	7.7	41.7± 1.3	
18_46	3.7	42.5± 0.5	
19_46	3.8	41.7± 0.3	
13H_1	23.4	41.7± 0.5	Si and Mn homogenized
17H_30	4.1	42.5± 0.6	" " " "

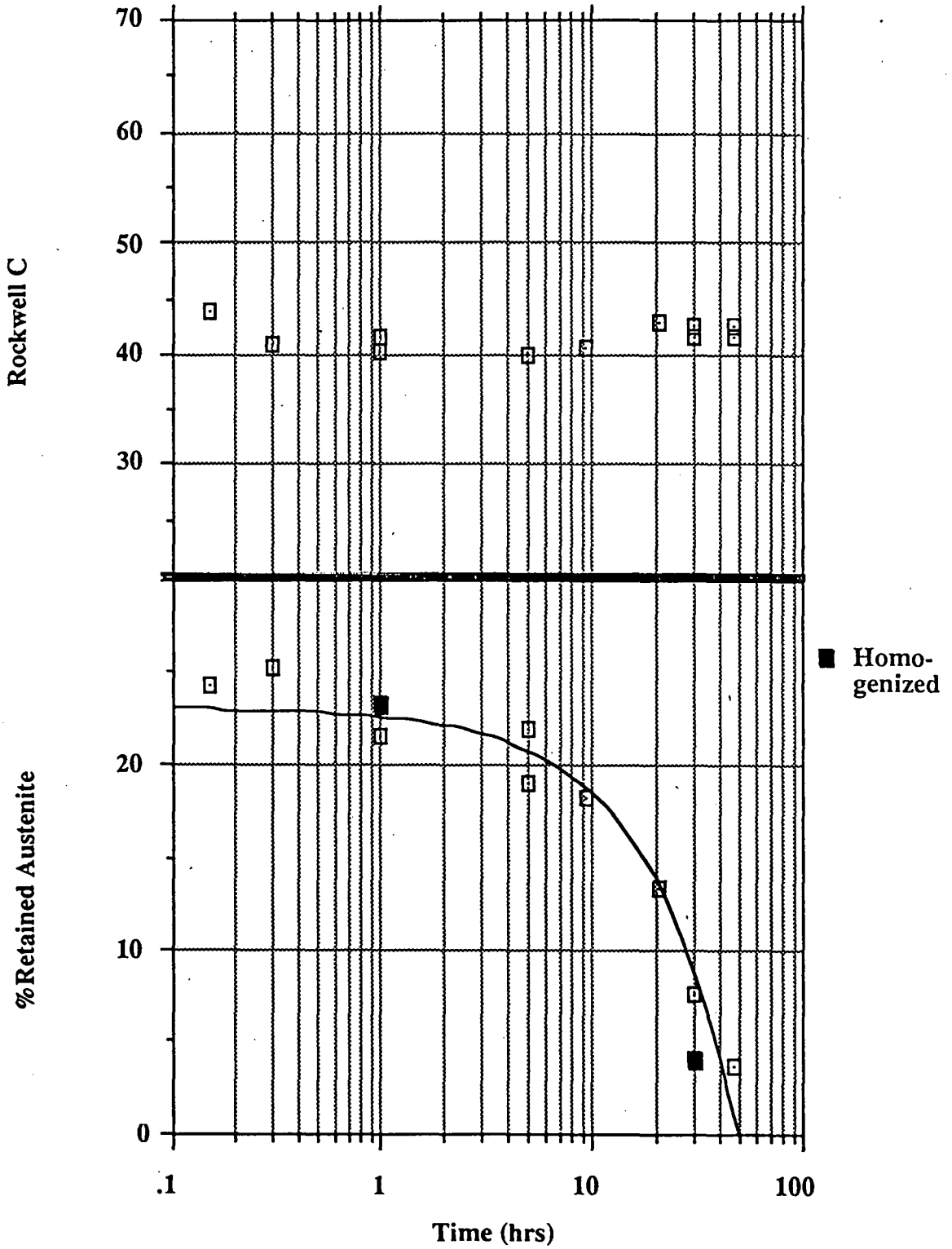

Figure 4. % R_γ and R_c versus time for the 1.0% Mn alloy KHB

Table 8. Results of Retained Austenite experiments using 2.0% Mn alloy as a function of time plus R_c results

ALLOY KHC (Fe + 2.479 Si + .651 C + 1.99 Mn)

Sample	Vol. % R.A.	R_c	Condition/Comments
20A_013	15.9	61.2± 1.3	tempered for 8 min
20B_013	15.9	60.1± 2.4	tempered for 8 min
22A_075	42.0	34.5± 1.8	" " 45 min
22B_075	42.0	34.6± 3.6	" " 45 min
19A_2	46.4	31.0± 2.5	" " 2 hrs
19B_2	45.5	31.2± 1.0	" " " "
18A_6	48.9	27.6± 1.8	" " 5.5 hrs
18B_6	47.4	28.9± 2.5	" "
17A_24	44.5	25.5± 2.8	" " 24 hrs
17B_24	45.9	27.6± 2.0	" " " "
21A_48	34.2	31.8± 2.2	" " 48 hrs
21B_48	32.2	32.1± 2.6	" " 48 hrs
23_96	13.5	41.3± 1.1	
24_30	32.38	37.5± 1.3	
25_72	17.81	41.0± 0.7	
26_144	12	42.0± 0.7	
27_18	40.65	36.9± 1.6	
28_03	28.76	56.6± 1.3	
19A_2X3	36.2	30.7± 1.3	repeat some of the
18A_6X3	41.6	29.0± 3.5	above samples
27_18X3	38.3	35.4± 0.4	
17A_24X3	41.9	28.8± 1.3	
24_30X3	32.8	35.0± 0.9	

Table 9. Results of Retained Austenite experiments using 2.0% Mn alloy as a function of time plus R_c results

ALLOY KH2C (Fe + 2.5 Si + .782 C + 2.0 Mn)			
Sample	Vol. % R.A.	R_c	Condition/Comments
31_015	19.0	64.1± 0.2	
32_05	24.3	61.8± 0.6	
33_1	38.1	54.1± 2.2	
34_4	49.9	38.1± 0.3	
35_9	51.8	37.1± 1.0	
36_19	50.2	38.4± 0.4	
37_32	40.7	39.3± 1.5	
38_51	27.4	42.3± 0.4	
39_101	24.0	42.4± 0.5	
34H_4	52.0	39.9± 0.8	Si and Mn homogenized
39H_101	17.6	31.4± 1.6	" " " "

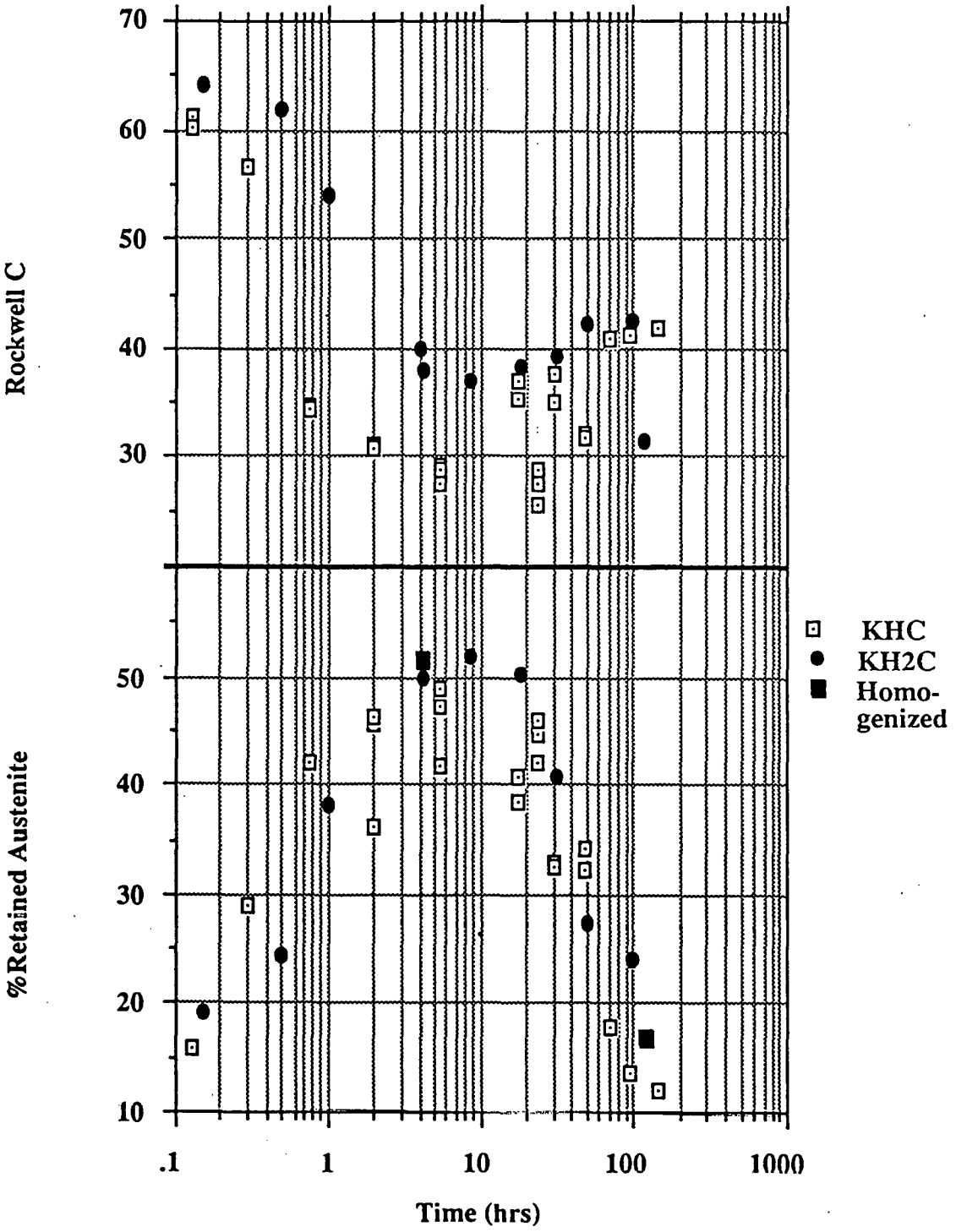

Figure 5. % $R\gamma$ and R_c versus time for the 2.0% Mn alloys KHC and KH2C

Table 10. Results of Retained Austenite experiments using 3.0% Mn alloy as a function of time plus R_c results

ALLOY KHD (Fe + 2.441 Si + 0.726 C + 3.04 Mn)

Sample	Vol. % R.A.	R_c	Condition/Comments
1_72	19.6	59.3± 2.2	
2_5	15.4	---	
2E_5	14.9	62.2± 0.4	EP 10 min no effect (also
3_48	19.9	59.4± 1.1	d2 & b16)
4_144	20.2	59.6± 0.5	
5_015	14.4	60.7± 1.0	
6_20	19.9	60.8± 1.3	
7_29	19.4	60.9± 0.7	
8_120	16.9	59.4± 0.9	
9_05	16.8	61.3± 0.8	
3H_48	15.3	60.9± 1.1	Si and Mn homogenized
4H_144	14.8	61.4± 1.8	" " " "

Table 11. Results of Retained Austenite experiments using 3.0% Mn alloy as a function of time plus R_c results

ALLOY KH2D (Fe + 2.5 Si + 0.728 C + 3.0 Mn)			
Sample	Vol. % R.A.	R_c	Condition/Comments
15_015	33.5	60.3± 1.2	
16_05	33.9	61.6± 0.4	
17_4	29.5	60.8± 0.6	
18_10	29.4	61.5± 0.3	
19_21	32.2	61.2± 0.2	
20_76	28.9	60.3± 0.4	
21_145	30.3	61.2± 0.1	w/o peak 8
22_261	29.9	58.6± 0.5	
23_504	27.0	58.0± 2.2	
16H_05	26.0	62.1± 0.1	Si and Mn homogenized
21H_145	29.3	61.2± 0.1	" " " "

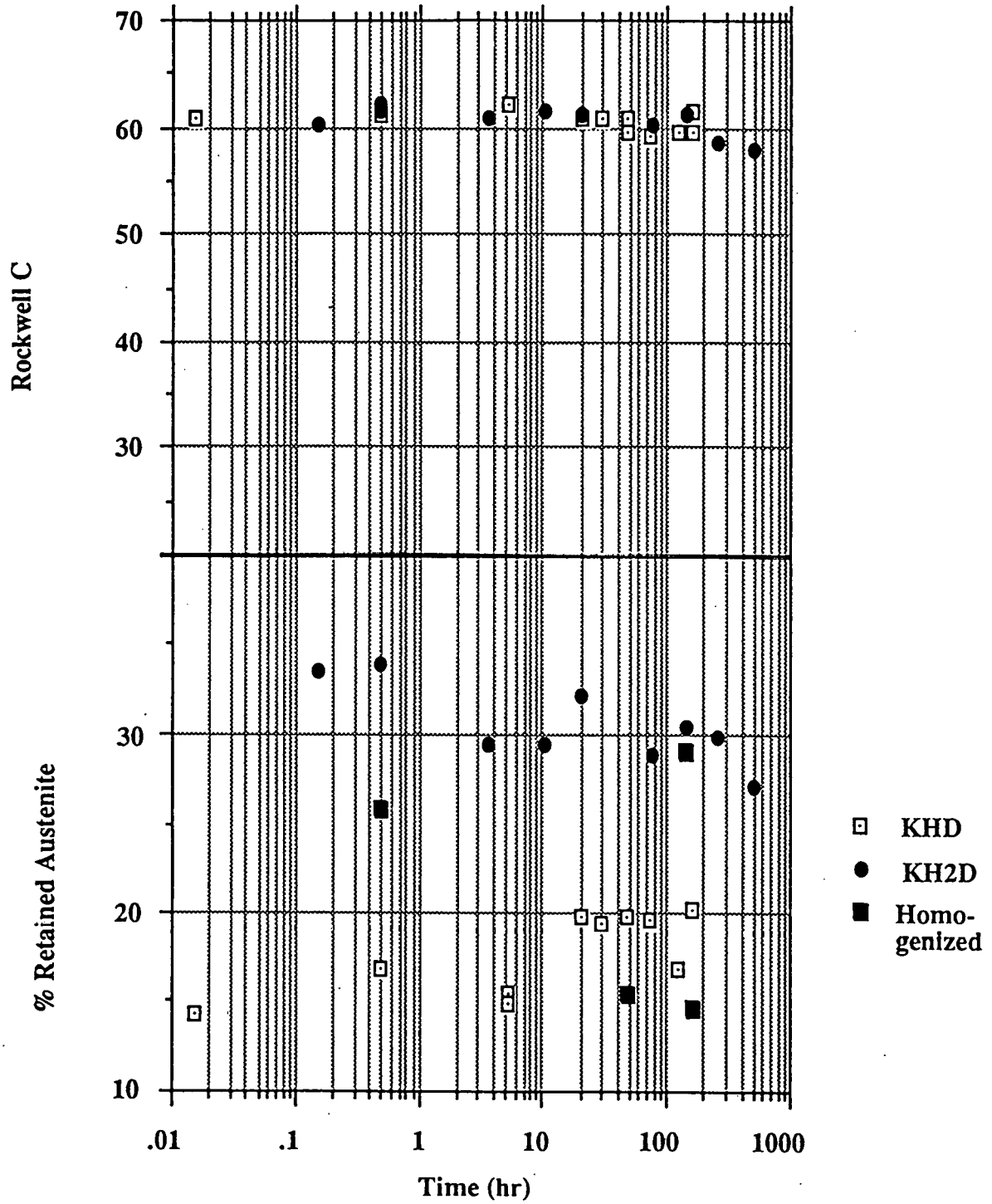

Figure 6. % R_γ and R_c versus time for the 3.0% Mn alloys KHD and KH2D

weeks of austempering.

The main goal of this research was to establish the onset times for the stage II reaction as a function of Mn content. Stage II occurs when carbides begin to form and is recognized here by a sharp decline in $R\gamma$ as a function of austempering time. The stage II onset times are listed in Table 12 and plotted in Figure 7. These onset times were chosen as the time at which the $R\gamma$ dropped to one half of it's maximum value.

C. Microstructural Evaluation

Figures 8 and 9 show typical microstructures resulting from the austempering process. Austempering is a two step process: 1) complete transformation to the (FCC) or austenite (γ) phase and 2) a quench and hold in the temperature range of 270-420° C for some time followed by cooling to room temperature. This quench must be sufficiently rapid to avoid formation of pearlite or ferrite if the best mechanical properties are to be obtained. Recall the two stages that occur in the austempering transformation. Firstly, the original austenite (γ_0) decomposes into bainitic ferrite (α) and high carbon austenite (γ_{HC}).

$$\text{Stage I :} \qquad \gamma_0 \longrightarrow \alpha + \gamma_{HC} \qquad (1)$$

The high carbon austenite later decomposes into bainitic ferrite plus carbide in the second stage.

$$\text{Stage II:} \qquad \gamma_{HC} \longrightarrow \alpha + \text{carbides.} \qquad (2)$$

Stage II is undesirable and is always avoided for industrial applications. These four micrographs taken after stage I is partially

Table 12. Stage II onset times for an austempering temperature of 370° C

Alloy designation	%C	%Si	%Mn	Onset time
KHA	.676	2.475	.291	8 hours
KHB	.709	2.454	1.00	25 hours
KHC	.651	2.479	1.99	40 hours
KHD	.726	2.441	3.04	>> 3 weeks
KH2C	.782	2.5[a]	2.0[a]	40 hours
KH2D	.728	2.5[a]	3.0[a]	>> 3 weeks

[a]Target composition.

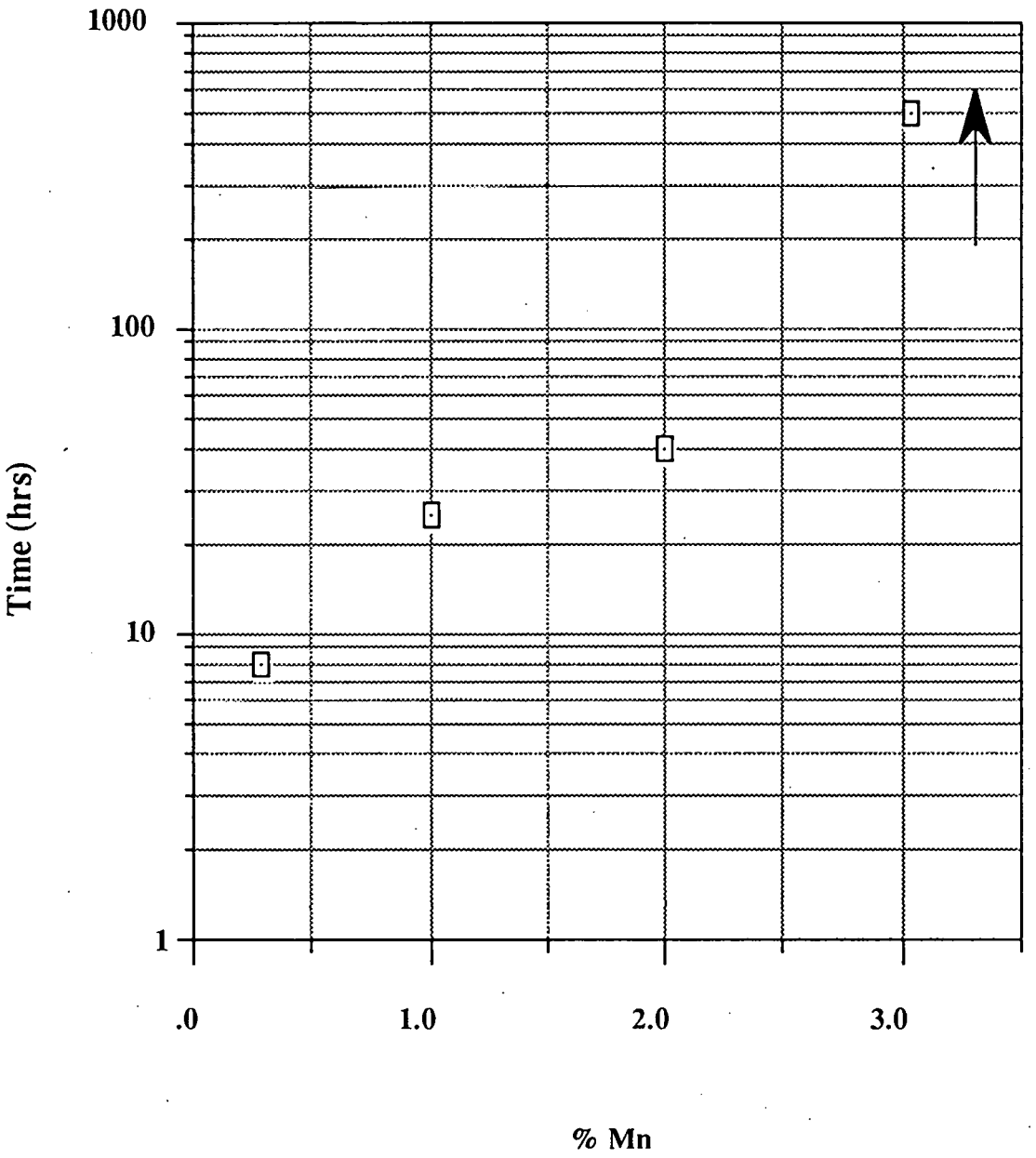

Figure 7. Stage II onset times vs % Mn

Figure 8. Optical micrographs of sample KHA48 austempered at 370° C for 4 hours (Nital etch) Magnifications: Top=100X, Bottom = 500X

Figure 9. Optical micrographs of sample KHB16 austempered at 370° C for 5 hours (Nital etch) Magnifications: Top=100X, Bottom = 500X

completed demonstrate that γ_{HC} plus bainitic ferrite are present at the salt bath temperature of 370° C. Because the martensite start temperature (M_S) is below room temperature the γ does not transform to martensite upon quenching to room temperature. Therefore, the room temperature microstructures shown in figure 8 and 9 contain bainitic ferrite (dark) plus Rγ (white). Alloys KHA and KHB contain these typical microstructures for all austempering times.

Figure 10 shows the type of microstructure observed for partial stage I completion in alloy KHC. Again the bainitic ferrite is dark and the Rγ white. Also apparent at low magnification (Figure 10 top) are segregation effects. The bainitic ferrite has formed in bands where, presumably, the Mn concentration is lower than the overall average Mn composition. At higher magnifications a large amount of Rγ is observed to have formed in pools. There is also Rγ which is not visible optically between the ferrite laths.

The 3% Mn alloy gave unexpectedly high R_c values (see figure 6). Metallographic examination of KHD and KH2D showed a very different microstructure than was observed in the previous three alloys. Figure 12 shows classical plate martensite in an γ matrix separated by bands of a dark etching phase. Figure 11 (top) shows the very pronounced banding present, which is likely the result of Mn and Si segregation. It was suspected that the dark etching phase was bainitic ferrite because α etches most rapidly with Nital and therefore appears dark in the optical microscope. Further experiments on the Scanning Electron Microscope (SEM) were done to confirm this suspicion. Figure 13 shows a region of the dark phase set off by fiducial microhardness marks at two

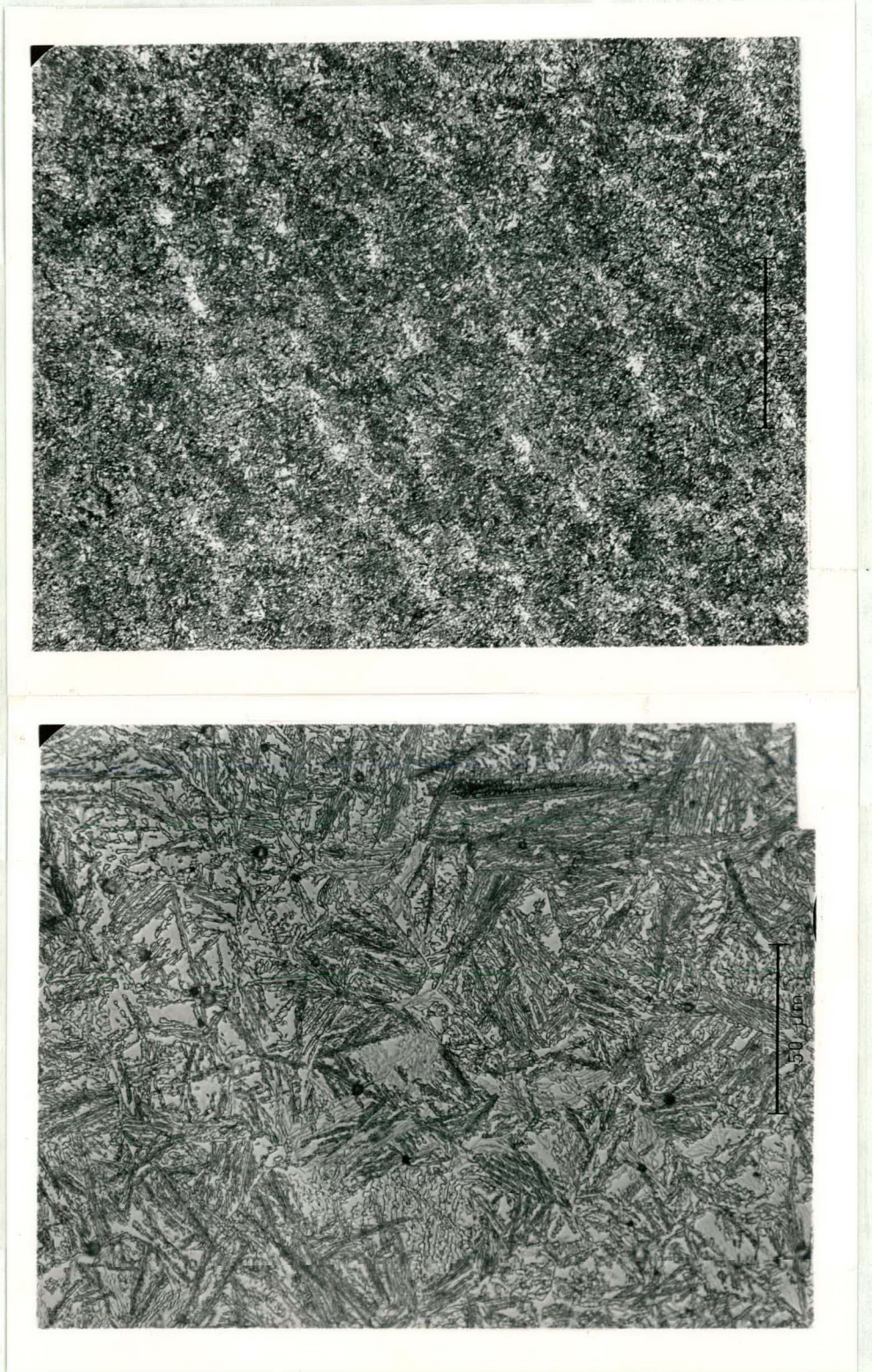

Figure 10. Optical micrographs of sample KHC18A austempered at 370° C for 5.5 hours (Nital etch) Magnifications: Top = 50X, Bottom = 500X

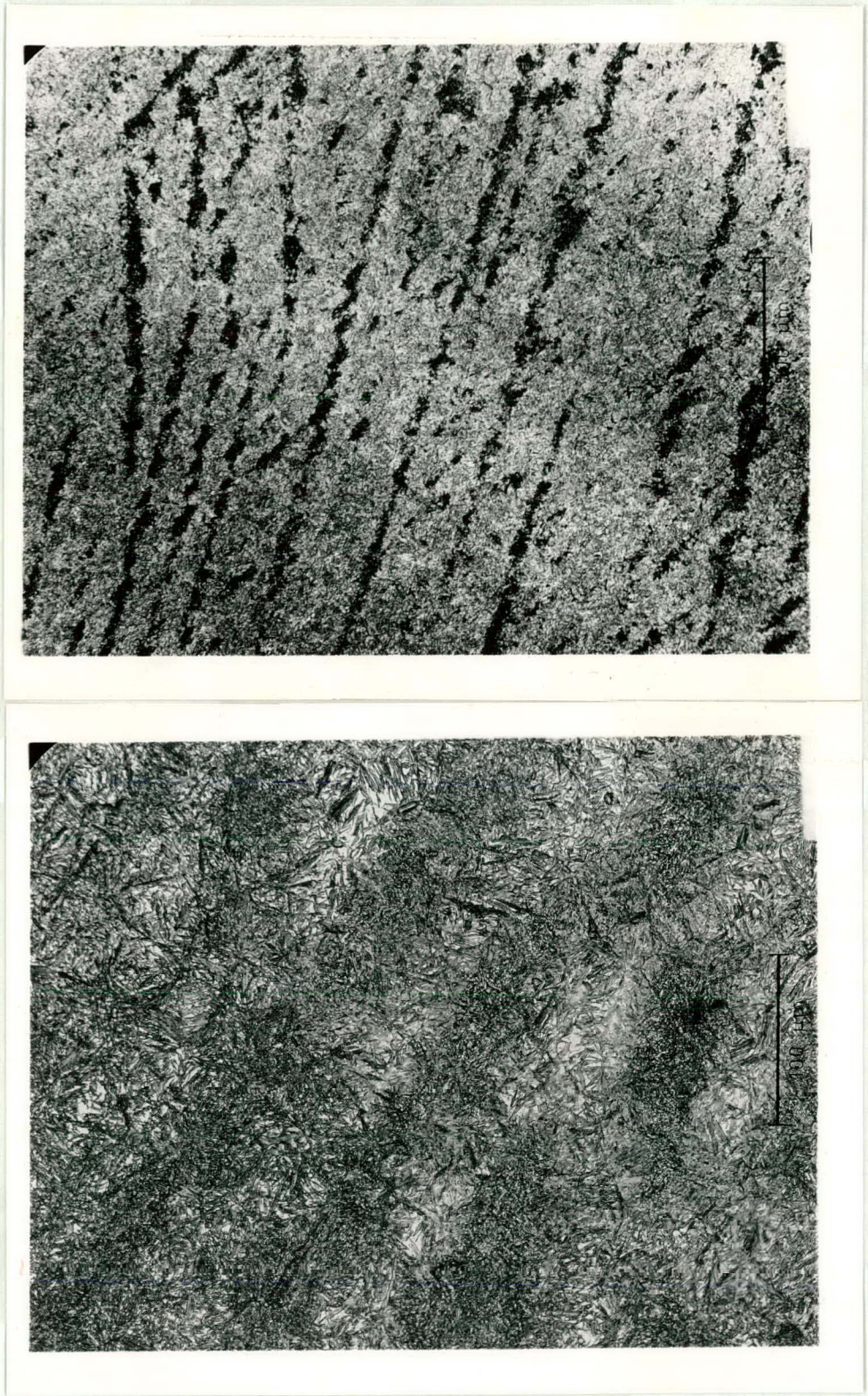

Figure 11. Optical micrographs of sample KH2D23 austempered at 370° C for 504 hours (Nital etch) Magnifications: Top=50X, Bottom = 250X

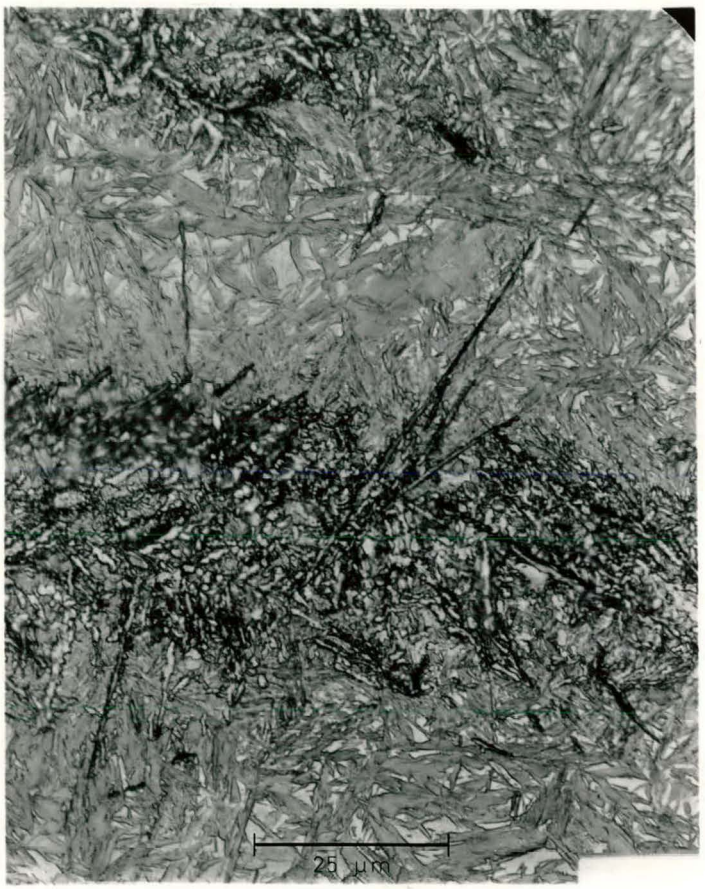

Figure 12. Optical micrograph of sample KH2D23 austempered at 370° C for 504 hours (Nital etch) Magnification: 1000X

magnifications in the optical microscope. In Figure 14 the same area was examined with the SEM. These pictures clearly show the dark phase to have etched out in the Nital and give strong evidence that it is bainitic ferrite.

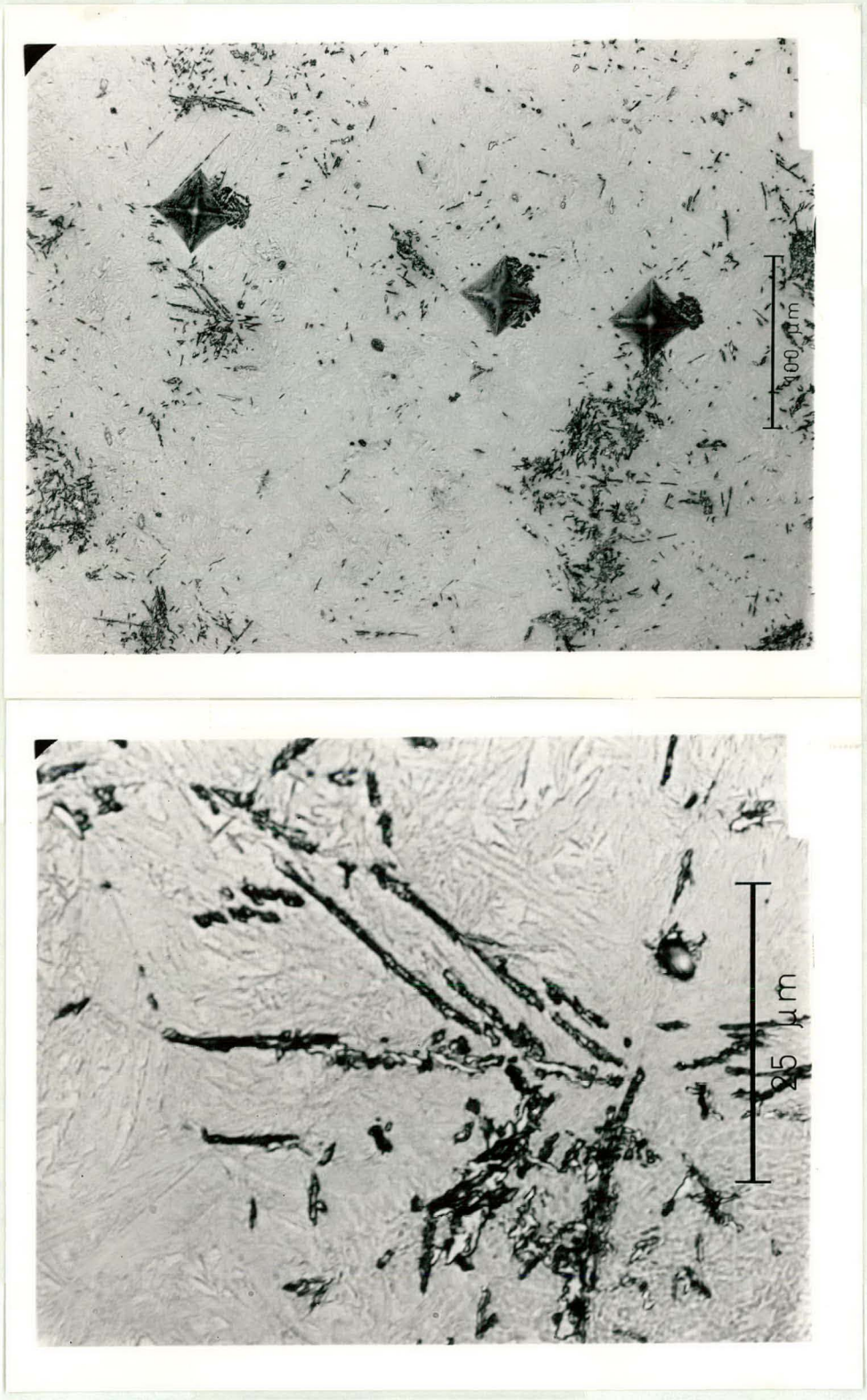

Figure 13. Optical micrographs of sample KH2D23 austempered at 370° C for 504 hours (Etch: .5% Sodium metabisulfite, 49.5% water, 2% Picric acid,48% Alcohol) Magnifications: Top=200X,Bottom=1800X

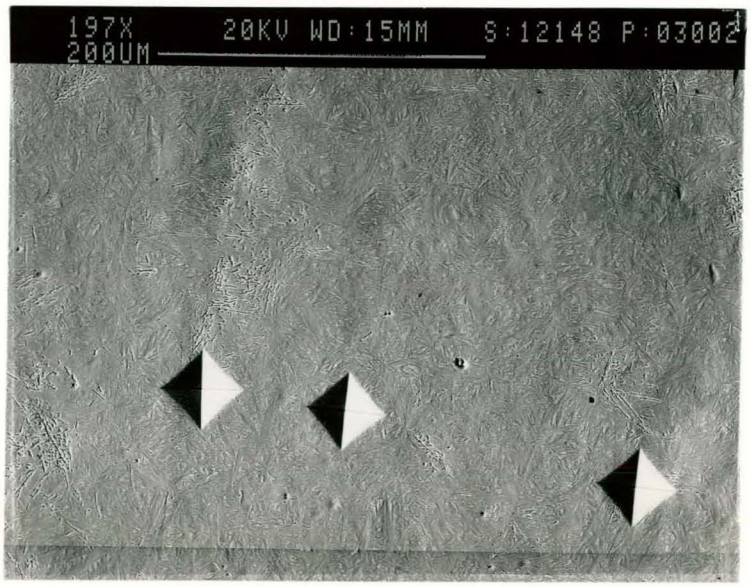

Figure 14. SEM micrographs of sample KH2D23 austempered at 370° C for 504 hours (Nital etch) Magnifications: Top=197X,Bottom=1790X

IV. SUMMARY and CONCLUSIONS

It is felt that the scatter in the early (Tables 3-5) $R\gamma$ data was due to a combination of two effects; a decarburization at the surface as a result of a relatively poor vacuum coupled with a strong sensitivity of $R\gamma$ to %C at values of %C close to the target value of 0.7% used in this work. That is, small differences in carbon level due to different amounts of decarburization as a result of positioning in the furnace were responsible for large $R\gamma$ variations. This problem was overcome by using improved vacuum techniques and by grinding 10 mils from the surface of all sample prior to measuring $R\gamma$. The idea that C level is extremely critical is supported by some unpublished research on Fe-C-Si alloys austempered at 420° C. Alloys of 2.5% Si, 0.4, 0.65, and 0.71% C were examined and the maximum $R\gamma$ values occurred for 420° C austempering times of around one minute giving values of 4.7%, 21.0% and 26.0% $R\gamma$ at 0.4, 0.65 and 0.71% C respectively, see Figure 15. Hence, it is likely that decarburization of the alloys used in this work (which were austempered at 370° C) from an initial 0.7% C to as low as 0.4% C accounts for the large scatter found in the initial studies. For example in Table 3 set 2, sample 4 (16% $R\gamma$, i.e. little decarburization) compared with sample 19 (4% $R\gamma$, i.e. decarburized to about 0.4% C) and the .4%C-2.5%Si-Fe alloy also containing only 4% $R\gamma$. A proposed relationship for %C vs %$R\gamma$ for two austempering temperatures is shown graphically in Figure 15. The five points plotted are from the data mention above and data from the present study. If the proposed curves are correct, then it is clear that only small changes in %C near the

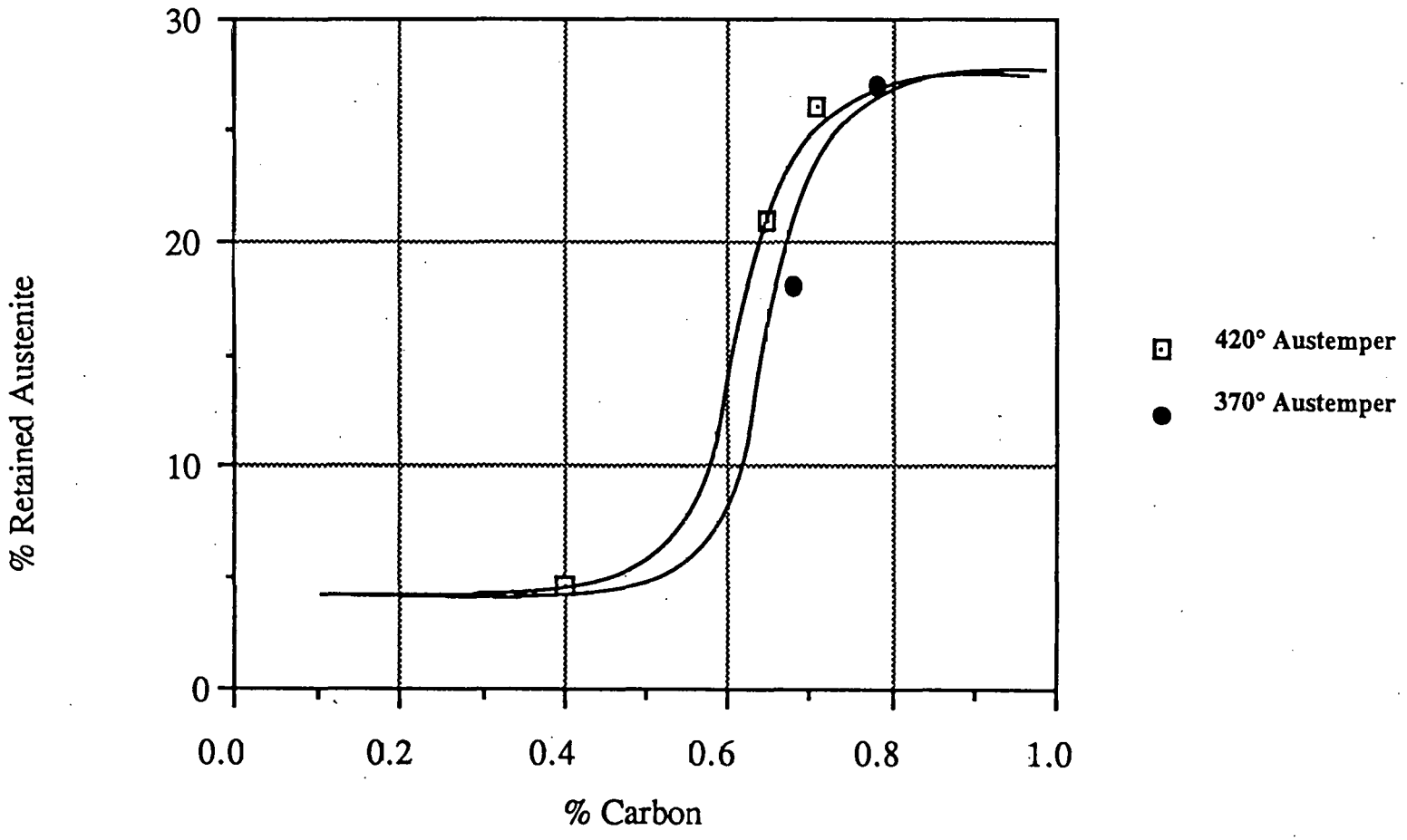

Figure 15. Proposed relationship for % C vs maximum % R_γ at 370° C and 420° C

0.7% level will lead to large changes in R_γ .

The accuracy of the texture determinations is quite good, reproducing measurements to about $\pm$ 0.02 in σ_p. Six R_γ measurements of sample 7 in Table 5 yielded R_γ = 29.96% $\pm$ 0.32%. Measurements were also made on two Fe-Ni-Cr NBS standards. An average measured value of 30% is compared to the 32.04% $\pm$ 0.5% guaranteed by NBS, and an averaged measured value of 5.1% for a 5.19% $\pm$ 0.25% NBS standard. It was therefore concluded that the accuracy of the present experimental technique was reasonable good.

The stage II onset times were delayed to an even greater extent than initially anticipated. For the alloys containing < 2% Mn stage II occurred after 8-40 hours of tempering at 370° C. In the case of KHD, the presence of 3% Mn stopped the formation of bainitic ferrite for all practical purposes. This dramatically demonstrates the significance of knowing when Mn segregation is present. In a highly segregated alloy local concentrations of Mn may be as high as 3%. As demonstrated, upon heat treatment, martensite will form in these areas with deleterious effects (see Figure 12).

While the magnitude of R_γ is lower than anticipated in KHA and KHB, the micrographs in Figures 8 and 9 show very typical austempering microstructures. It is believed that the lower amount of R_γ is due to a very strong dependence on carbon for the following reasons. Carbon content is the only compositional difference between KHDF and KHA, with KHDF having about 16% more C. Increasing the C in ordinary steels causes an increase in R_γ [5]. Samples from the two alloys were processed under identical conditions in several experiments (Tables 3

and 6) with KHDF containing considerably more $R\gamma$. KHB also has low C with respect to KHDF and the amount of $R\gamma$ is again lower than one might expect. However, the amount of $R\gamma$ in KHB is greater than in KHA because of the higher Mn content.

For KHC the effect of C is overshadowed by a large alloy content of Si+Mn = 4.5%. The micrographs in Figure 10 show segregation at low magnification and large areas (pools) of untransformed austenite at higher magnifications. The $R\gamma$ one expects to measure after austempering is located between the α laths as well as some pool γ . Here the additional formation of some pool γ causes a very large amount of $R\gamma$ to be measured. For KHC the Mn has slowed the transformation of γ to bainitic ferrite a great amount. However, bainitic ferrite is still forming in sufficient quantities and ejecting enough C into the γ to lower the M_S temperature to well below room temperature. At the termination of the 370° C temper the samples must contain ferrite plus a very high carbon austenite (with a corresponding low M_S) to produce the observed microstructure (see Figure 10).

In KHD the Mn content is so high that bainitic ferrite formation is almost halted. Because the bainitic ferrite is not forming, the C level in the γ is too low to drive the M_S below room temperature. The bainitic ferrite + γ microstructure existing at 370° C is transformed to bainitic ferrite + martensite + $R\gamma$ on cooling to room temperature. The reason that the $R\gamma$ does not show an increase with austempering time is that so little bainitic ferrite is forming (~ 10%) that the additional $R\gamma$ formed is only a few percent. This alloy also exhibits marked segregation. In the nonhomogenized samples the bainitic ferrite forms

in bands (dark regions in the upper micrograph of Figure 11). Bands were also evident in the martensite matrix (Figure 11 bottom). The dark bands have a $R_c \sim 56$, and the matrix has $R_c \sim 63$. These dark bands are presumably areas of lower Mn where bainitic ferrite is able to form. The segregation had little if any effect on the overall $R\gamma$ content, as shown in the 10 homogenized samples measured. This strengthens the hypothesis that C level is critical in determining the magnitude of $R\gamma$ at a given austempering temperature.

The alloying effects discussed here have dominated the reactions so that any surface preparation effects are difficult to observe. It is likely that the method of surface grinding 10 mils and then electropolishing at 0° C is the best choice, but one may wish to study this after the alloying effects are better understood.

The major results of this study are presented in Table 12 and Figure 7, where the onset time for the stage II reaction is shown to be a strong function of the Mn level. Another important result of this study is that at low Mn levels, under 1% Mn, the amount of $R\gamma$ is apparently a strong function of % C for levels of % C in the 0.4 to 0.8% range. Additional experiments need to be done to determine this dependence.

V. REFERENCES

1. A. L. Hitchcox, Met. Prog., 130, 49, (August 1986).

2. R. B. Gundlach and J. F. Janowak, Met. Prog., 128, 19, (July 1985).

3. Proc. 1st Int. Conf. on Austempered Ductile Iron, American Society of Metals, Metals Park, OH, 1984.

4. L. L. Jones, M.S. Dissertation, Iowa St. Univ., Ames, Iowa, 1985.

5. J. D. Verhoeven, Fundamentals of Physical Metallurgy, John Wiley and Sons, New York, 1975.

6. J. D. Verhoeven and H. L. Downing, J. Heat Treat., 6, 21, (1988).

7. B. D. Cullity, Elements of X-Ray Diffraction, Addison-Wesley Publ. Co., Reading, MA, 1978.

8. J. Durnin and K. A. Ridal, J. Iron Steel Inst., 206, 60 and 1035, (1968).

9. C. F. Jatczak, J. A. Larson and S. W. Shin, Retained Austenite and its Measurement by X-Ray Diffraction, SP-453, Society of Automotive Engineers, Inc., Warrendale, PA, January 1980.

10. M. J. Dickson, J. Appl. Crystallogr., 2, 176, (1969).

11. J. D. Verhoeven and D. P. Cornwell, unpublished research, Ames Laboratory, Ames, IA (1985).

VI. ACKNOWLEDGEMENTS

I want to thank God through whom all things are possible.

I am especially grateful to my major professor, Dr. John D. Verhoeven, for his encouragement and guidance. He is an insightful researcher and the best teacher I have had in my 20 years of school.

Underneath the research and technical work must lie a strong foundation of perseverance and dedication that was learned at a very early age. I am forever indebted to my parents for their encouragement and unwavering support.

Special thanks are due Ed Gibson, Les Reed, Harlan Baker, and Ardis Johnson whose technical assistance was invaluable.

I'm also indebted to Tom Wessels for his help writing the computer software.

I also want to thank Park, Dan, Carole, Jeff, and Kevin for their friendship and encouragement.

Finally, I want to thank Nat for being my very special friend.

This work was funded in part by a John Deere Foundation grant. Thank you to John Deere for this support.

This work was performed at Ames Laboratory under contract No. W-7405-eng-82 with the U. S. Department of Energy. The United States government has assigned the DOE Report number IS-T-1394 to this thesis.